Materials Letters 220 (2018) 313–316

Contents lists available at ScienceDirect

Materials Letters

journal homepage: www.elsevier.com/locate/mlblue

Featured Letter

Synthesis of pyridinic-N doped carbon nanofibers and its electro-catalytic activity for oxygen reduction reaction

Min Sun [a], Xiaobo Wu [a,b], Xiaoting Deng [a], Wei Zhang [a], Zhiyong Xie [a,*], Qizhong Huang [a,*], Boyun Huang [a]

[a] *State Key Laboratory of Powder Metallurgy, Central South University, 932 Lushan Road, Changsha 410083, PR China*
[b] *School of Metallurgical Engineering, Hunan University of Technology, Zhuzhou, Hunan 412008, PR China*

ARTICLE INFO

Article history:
Received 3 January 2018
Received in revised form 19 February 2018
Accepted 8 March 2018
Available online 9 March 2018

Keywords:
Carbon materials
Microstructure
Active sites
Oxygen reduction reaction
Nitrogen doping
Chemical vapor deposition

ABSTRACT

As catalytic active sites of nitrogen (N)-doped carbon nanomaterials (CNMs) for oxygen reduction reaction (ORR) are always under debate, synthesis of high purity pyridinic-N dominated CNMs is an effective approach to study the relation between pyridinic-N and active sites, as well as catalytic mechanism for ORR. Herein, the carbon nanofibers (CNFs) etched by hydrofluoric (HF) acid can be used to synthesize pure pyridinic-N, suggesting that the exposed edge-patterned surface facilitates to synthesize pure pyridinic-N. Moreover, it reveals that the carbon atoms adjacent to pyridinic-N could be the catalytic active sites for ORR.

1. Introduction

Fuel cells have been considered as an ideal and clean energy-converting device [1,2]. N-doped CNMs have become the most promising candidates for the high-cost and scarce Pt-based catalysts, due to their low-cost and excellent electrochemical activity for ORR [3–5].

In order to fabricate high-performance ORR catalysts, N-doped CNMs should be synthesized with higher concentration of active sites. Studies show that the doping N atoms generally exhibit four bonding configurations, pyridinic-N, pyrrolic-N, graphitic-N and oxidized-N. And pyridinic-N facilitating to create catalytic active-sites is confirmed by many reports [3,6–8]. However, this opinion needs to be further demonstrated, in consideration of mixing N bonding configurations in as-synthesized catalysts [9]. Therefore, it is imperative and crucial to synthesize high purity pyridinic-N doping CNMs [3,6,7].

As the pyridinic-N prefers to locate at the edge sites of CNMs [6], an edge-patterned surface of CNMs with inner intact six-membered ring seems to be essential for synthesizing high purity pyridinic-N. Guo etc. [6] synthesized pyridinic-N doped highly oriented pyrolytic graphite (HOPG) via NH_3 post-treatment. Considering that CNFs are all composed of graphite crystallite and possess abundant edge sites, it could be speculated logically that CNFs hold great promise to be used for synthesizing pure pyridinic-N [3]. In general, CNFs possess several microstructures, porous CNFs (pCNFs), platelet CNFs (plCNFs) and fish-bone CNFs (fCNFs) [10].

In our previous work, we have synthesized pyridinic-N doped plCNFs and investigated the nitrogen doping mechanism [3]. In this work, we mainly investigated the effects of microstructure of CNFs (namely fCNFs, plCNFs and pCNFs) on N doping and the catalytic activity for ORR.

2. Experiments

Firstly, the fCNFs, plCNFs and pCNFs were in-situ synthesized on carbon paper (CP) surface via chemical vapor deposition (CVD). Secondly, the pyridinic-N doped CNFs were prepared via post-treatment the edge-patterned CNFs, which were obtained by HF etching CNFs, under NH_3 atmosphere and they were denoted as N-fCNFs, N-plCNFs and N-pCNFs, respectively (the details are shown in ESI).

3. Characterization

The as-prepared samples are characterized by SEM, TEM (HRTEM), XPS, Raman spectroscope. The electro-chemical tests were performed in 0.1 M O_2/N_2 saturated KOH solution at a scan

---

* Corresponding authors.
E-mail addresses: xzy507@csu.edu.cn (Z. Xie), qzhuang@csu.edu.cn (Q. Huang).

https://doi.org/10.1016/j.matlet.2018.03.050
0167-577X/

rate of 10 mV s^{-1} via a standard three-electrode cell (the details are shown in ESI).

4. Results and discussions

Fig. 1a–c are typical TEM images which are used to illustrate the distinctive structures of fCNFs, plCNFs, and pCNFs. With increasing the concentration of the carbon feedstock, the microstructure of CNFs transform from fCNFs, to plCNFs, and to pCNFs, which is due to the synergistic effect of several factors, such as C—C bond energy, the diffusion barriers of carbon atoms in nickel catalysts and so on [10,11]. Moreover, Fig. 1d–i demonstrate that various CNFs are composed of graphite crystallites, which are arranged in different ways. Additionally, it can be observed that the adjacent graphene sheets are closed at the outer edge sites of CNFs (Fig. 1d–f insets red dotted rectangles), resulting in the elimination of the carbon dangling bonds and forming closed loop structures [3,12]. However, the closed loop structures could be broken down via HF etching, generating an exposed edge sites at outer surface of CNFs (Fig. 1g–i insets red dotted rectangles).

The specific surface areas of N-fCNFs (77.23 $m^2\,g^{-1}$), N-plCNFs (84.56 $m^2\,g^{-1}$) and N-pCNFs (76.98 $m^2\,g^{-1}$) increase compared with that of fCNFs (51.73 $m^2\,g^{-1}$), plCNFs (59.62 $m^2\,g^{-1}$) and pCNFs (49.53 $m^2\,g^{-1}$), suggesting that the exposed edge sites and ratio of boundary atoms increasing. This result is in an accordance with the Raman spectra (Fig. S3): The I_D/I_G values of the samples also indicate that the exposed patterned-edge planes increase in N-fCNFs, N-plCNFs and N-pCNFs, compared with those in the corresponding fCNFs, plCNFs and pCNFs. The obvious intensive C, N, and weaker O signals are presented in the XPS spectra (Fig. 2a). In Fig. 2d–f, the N1s XPS spectra with one sharp signal are fitted with pure pyridinic-N bonding configuration, suggesting pure pyridinic-N synthesized successfully. As plCNFs possess the most exposed nitrogen doping sites, N-plCNFs have the highest concentration of pyridinic-N (12.61 at.%) (Fig. 2b). Meantime, the N bonding configurations in N doped untreated CNFs (denoted as N_m-CNFs) were also investigated, indicating lower N content and mixing N types (Fig. S4). Furthermore, XPS spectra of N-CNFs before and after ORR (Fig. 2) are investigated to figure out what the catalytic-active sites for ORR are. The C and N bonding configurations vary obviously after ORR (Fig. 2b and c), and pyridinic-N decreases while the peak signal at 399.9 eV appears (Fig. 2). To study the N type at 399.9 eV, the C1s XPS spectra of the N-CNFs before and after ORR are also investigated (Fig. S2). It reveals that the C(aromatic)-OH (at 285.4 eV) [9] relatively increases after ORR for all samples, suggesting that the N1s XPS peak at 399.9 eV after ORR probably could be pyridone-N, rather than pyrrolic-N. As a conclusion, the carbon atoms adjacent to pyridinic-N tend to react with –OH species (forming pyridone-N) during ORR, and it could be speculated reasonably that the carbon atoms next to pyridinic-N could facilitate the catalytic active sites rather than pyridinic-N itself, which is in accordance with the results in Refs [6,9].

Fig. 3 schematically exhibits the closed loop structures of CNFs and the open edge sites in various N-CNFs, respectively. Comparing with the inner graphene layer with intact six-membered ring structure (Fig. 3a and h), the closed loop structure is composed of six-membered rings, and five-membered rings with defects (Fig. 3a and j), which are of disadvantage to the generation of high purity pyridinic-N [3]. In this paper, we design a novel and facile approach to tailor the disordered closed loop structure, forming an ideal carbon substrate with inner intact six-membered ring structure and exposed edge-patterned sites, which provides abundant potential doping sites for pyridinic-N (Fig. 3b, d, and f). Although graphene sheets are arranged in different ways for fCNFs, plCNFs, and pCNFs, they could be served as high purity pyridinic-N doping model and the reasons are deduced as following: Firstly, the graphene sheets are stacked differently in the fCNFs, plCNFs, and pCNFs, however, they are all composed of graphite crystalline with intact six-membered ring structure; Secondly, the chaotic edge planes of the CNFs are etched by HF, forming more open and protuberant patterned-edge sites, where the pyridinic-N prefers to locate; Thirdly, nitrogen atoms hardly enter into the

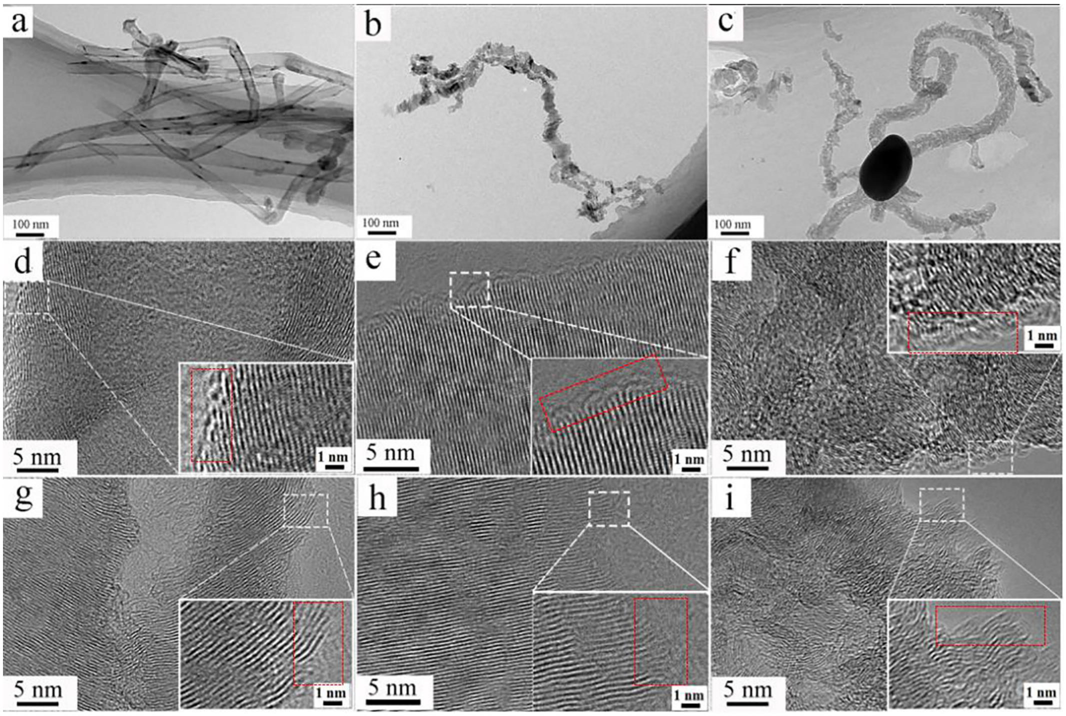

Fig. 1. TEM and HRTEM images of the as-prepared samples. (a) and (d) fCNFs, (b) and (e) plCNFs, (c) and (f) pCNFs; (g) fCNFs, (h) plCNFs and (i) pCNFs etched by HF.